

RESEARCH ARTICLE

A pilot study: Nano-hydroxyapatite-PEG/PLA containing low dose rhBMP2 stimulates proliferation and osteogenic differentiation of human bone marrow derived mesenchymal stem cells

Eda Çiftci Dede^{1,2}  | Merve Gizer³  | Feza Korkusuz⁴ | Zeynep Bal⁵ |
Hiroyuki Ishiguro⁶ | Hideki Yoshikawa⁷ | Takashi Kaito⁸  | Petek Korkusuz⁹ 

¹Department of Bioengineering, Graduate School of Science and Engineering, Hacettepe University, Ankara, Turkey

²AO Research Institute Davos, Davos, Switzerland

³Department of Stem Cell Sciences, Graduate School of Health Sciences, Hacettepe University, Ankara, Turkey

⁴Department of Sports Medicine, Faculty of Medicine, Hacettepe University, Ankara, Turkey

⁵Signal Transduction, Immunology Frontier Research Center (IFReC), Osaka University, Osaka, Japan

⁶Department of Orthopaedic Surgery, National Hospital Organization Osaka National Hospital, Osaka, Japan

⁷Department of Orthopaedic Surgery, Toyonaka Municipal Hospital, Osaka, Japan

⁸Orthopaedic Surgery, Osaka University, Osaka, Japan

⁹Department of Histology and Embryology, Faculty of Medicine, Hacettepe University, Ankara, Turkey

Correspondence

Takashi Kaito, Department of Orthopaedic Surgery, Osaka University Graduate School of Medicine, Osaka, Japan.

Email: takashikaito@ort.med.osaka-u.ac.jp

Abstract

Background: Bone morphogenetic protein 2 (BMP2) can enhance posterolateral spinal fusion (PLSF). The minimum effective dose that may stimulate mesenchymal stem cells however remains unknown. Nano-hydroxyapatite (nHAp) polyethylene glycol (PEG)/polylactic acid (PLA) was combined with recombinant human BMP2 (rhBMP2). We in vitro evaluated proliferation, differentiation, and osteogenic genes of human bone marrow mesenchymal stem cells with 0.5, 1.0, and 3.0 µg/mL rhBMP2 doses in this study.

Methods: In vitro experimental study was designed to proliferation by a real-time quantitative cell analysis system and the osteogenic differentiation by alkaline phosphatase (ALP) activity and osteogenic marker (Runx2, OPN, and OCN) gene expressions of human derived bone marrow mesenchymal stem cells (hBMMSCs). nHAp was produced by wet chemical process and characterized by Fourier transform infrared spectrophotometer, scanning electron microscopy, and energy-dispersive x-ray spectroscopy. PEG/PLA polymer was produced at a 51:49 molar ratio. 0.5, 1.0, and 3.0 µg/mL rhBMP2 and nHAp was combined with the polymers. hBMMSCs were characterized by multipotency assays and surface markers were assessed by flow cytometer. The hBMMSC-rhBMP2 containing nHAp-PEG/PLA composite interaction was evaluated by transmission electron microscopy. Proliferative effect was evaluated by real-time proliferation analysis, and osteogenic capacity was evaluated by ALP activity assay and qPCR.

Abbreviations: ALP, alkaline phosphatase; EDX, energy dispersive x-ray spectroscopy; FTIR, Fourier transform infrared spectroscopy; hBMMSCs, human bone marrow derived mesenchymal stem cells; HLA-DR, human leukocyte antigen-DR isotype; ITS, insulin transferrin selenous acid; nHAp, nano-hydroxyapatite; OCN, osteocalcin; OPN, osteopontin; PEG, polyethylene glycol; PLA, polylactic acid; PLSF, posterolateral spinal fusion; qPCR, quantitative real time protein chain reaction; rhBMP2, recombinant human bone morphogenetic protein 2; Runx2, Runt-related transcription factor 2; SEM, scanning electron microscopy; SOX9, SRY-box transcription factor 9; TEM, transmission electron microscopy; TGF, transforming growth factor; µCT, microcomputer tomography.

Eda Çiftci Dede and Merve Gizer contributed equally as first authors.

This is an open access article under the terms of the [Creative Commons Attribution-NonCommercial-NoDerivs](https://creativecommons.org/licenses/by-nc-nd/4.0/) License, which permits use and distribution in any medium, provided the original work is properly cited, the use is non-commercial and no modifications or adaptations are made.

© 2023 The Authors. *JOR Spine* published by Wiley Periodicals LLC on behalf of Orthopaedic Research Society.

Petek Korkusuz, Histology and Embryology,
Faculty of Medicine, Hacettepe University,
Ankara, Turkey.
Email: petek@hacettepe.edu.tr

Funding information

Japan Society for the Promotion of Science;
Türkiye Bilimsel ve Teknolojik Araştırma
Kurumu

[Correction added on 23 June 2023, after first
online publication: Petek Korkusuz was added
as co-corresponding author]

Results: hBMMSC proliferation in the 0.5 µg/mL rhBMP2 + nHAp-PEG/PLA and the 1.0 µg/mL rhBMP2 + nHAp-PEG/PLA groups were higher compared to control. 1.0 µg/mL rhBMP2 + nHAp-PEG/PLA and 3.0 µg/mL rhBMP2 + nHAp-PEG/PLA containing composites induced ALP activity on days 3 and 10. 0.5 µg/mL rhBMP2 + nHAp-PEG/PLA application stimulated Runx2 and OPN gene expressions.

Conclusion: rhBMP2 + nHAp-PEG/PLA composites stimulate hBMMSC proliferation and differentiation. The nHAp-PEG/PLA composite with low dose of rhBMP2 may enhance bone formation in future clinical PLSF applications.

KEYWORDS

bone regeneration, mesenchymal stem cells, nano-hydroxyapatite, polyethylene glycol, polylactic acid, posterolateral spinal fusion, rhBMP2

1 | INTRODUCTION

Auto-, allo-, and synthetic- grafts are frequently used for posterolateral spinal fusion (PLSF).¹ Donor site morbidity and limited availability² restrict the use of autografts. Allografts on the other hand may trigger immune response³ and cause disease transmission.⁴ Bone morphogenetic protein 2 (BMP2) has been used clinically for PLSF⁵ to enhance bony fusion.⁶ High doses of recombinant human BMP2 (rhBMP2) caused side effects⁷⁻⁹ such as ectopic bone formation^{10,11} adipogenesis,¹² and osteoclast-mediated bone resorption. Recent research focused on decreasing the dose.¹³ A current study¹⁴ delivered BMP2/BMP6/activin A chimera with in a recombinant human collagen plus calcium-deficient hydroxyapatite porous composite matrix in monkeys for PLSF to overcome problems of supraphysiologic BMP2 concentrations. BMP2 combined with synthetic grafts including polymers,¹⁵⁻¹⁷ bioceramics,^{18,19} bioactive glass²⁰ and their composites²¹⁻²³ could facilitate adequate PLSF. The minimum effective rhBMP2 dose combined with synthetic grafts is however not determined.^{15,19,22-27} The in vitro induction and proliferation of human-derived bone marrow mesenchymal stem cells (hBMMSCs) with the minimum effective rhBMP2 dose is also open to discussion. Recent studies^{21-23,28-32} that combined rhBMP2 with biomaterials

worked in the range of 0.3 ng/mL and 250 µg/mL rhBMP2 doses (Table 1). Two recent studies^{21,33} reported proliferation of pre-osteoblasts and hBMMSCs with low dose of rhBMP2. Contradictory results on hBMMSCs proliferation stimulated by the release of rhBMP2 from synthetic grafts necessitated this in vitro study for PLSF. We worked with 0.5, 1.0, and 3.0 µg/mL as a threshold for the “low-dose rhBMP2” that was not defined. Nano-hydroxyapatite (nHAp) is osteoconductive³⁴ and could enhance rhBMP2 release from polylactic acid (PLA) and polyethylene glycol (PEG). nHAp also enhances cell adhesion by increasing the surface area of the composites.⁹ In vitro stimulation of hBMMSCs by rhBMP2 release from synthetic grafts was demonstrated in limited studies^{21,33} with controversial results.^{15,22-27} Five microgram¹⁵ and 200 µg/mL²² rhBMP-2 doped silk based composites did not affect alkaline phosphatase (ALP) activation of rat and human BMMSCs, however 1 µg/mL BMP2 doped PLA increased ALP, Runx2 and OPN expressions of rabbit²⁴ and human²⁶ BMMSCs. We previously produced and assessed a novel rhBMP2 containing nHAp-PEG/PLA in a rat PLSF model.³⁰ 150 ng (3.1%) and 300 ng (6%) of the 5 µg rhBMP2 released from the composite on days 1 and 21 in that study, respectively. Micro-computer tomography (µCT) revealed a higher bone and trabecular volume in 10 µg rhBMP2 group when compared to 3 µg

TABLE 1 Dose determination for rhBMP2, nHAp, and polymer composites.

Materials			
rhBMP2	nHAP	Polymer	References
2.5 and 250 µg/mL	✓	Silk fibroin/chitosan	28
200 µg/mL	✓	PLA-Collagen	23
20 µg	✓	PLGA-PEG-COOH	29
3.0 and 10 µg/mL	✓	PLA/PEG	30
0.5, 1.0, and 3.0 µg/mL	✓	(PLA/PEG)	Current study
0.5 µg/mL	✓	Ploxamer 407	31
0.2 µg/µL	✓	Silk-fibroin	22
0.1 µg/mL	✓	PLA-Collagen	32
0.3 ng/mL	✓	PLGA	21

rhBMP2 group. A more solid fusion mass and a higher bone volume to trabecular volume ratio was however evaluated with 3 μg rhBMP2. Manual palpation assessment in that study was the same in both groups.³⁰ In this current study, we further asked whether this novel rhBMP2 containing nHAp-PEG/PLA composite will stimulate proliferation and osteogenic differentiation of hBMSCs in vitro with 0.5, 1.0, and 3.0 $\mu\text{g}/\text{mL}$ rhBMP2 doses.

We aimed to evaluate adhesion by scanning electron microscopy (SEM), proliferation by an impedance based real time proliferation monitoring system, osteogenic differentiation properties by intracellular ALP activity and osteogenic activity related genes runt-related transcription factor 2 (Runx2), osteopontin (OPN) and osteocalcin (OCN) expressions by qPCR of 0.5, 1.0, and 3.0 $\mu\text{g}/\text{mL}$ rhBMP2 doses on hBMSCs after combining with nHAp-PEG/PLA.

2 | MATERIALS AND METHODS

2.1 | Design

An in vitro observational study was designed (Figure S1). Groups were (a) osteogenically induced hBMSCs (+ control), and (b) untreated hBMSCs (– control) control groups, (c) carrier nHAp-PEG/PLA, (d) 0.5 $\mu\text{g}/\text{mL}$ rhBMP2, (e) 1.0 $\mu\text{g}/\text{mL}$ rhBMP2, (f) 3.0 $\mu\text{g}/\text{mL}$ rhBMP2, (g) 0.5 $\mu\text{g}/\text{mL}$ rhBMP2 + nHAp-PEG/PLA, (h) 1.0 $\mu\text{g}/\text{mL}$ rhBMP2 + nHAp-PEG/PLA, (i) 3.0 $\mu\text{g}/\text{mL}$ rhBMP2 + nHAp-PEG/PLA experimental groups. Proliferation ($n = 3$) was assessed by an impedance based real time proliferation monitoring system (RTCA, xCELLigence, Agilent Scientific Instruments). ALP activity ($n = 6$) and osteogenic marker gene expressions for Runx2, OPN, and OCN using qPCR ($n = 3$) analysis with hBMSCs were undertaken for osteogenic differentiation. We reported the qPCR analysis results according to the MIQE guidelines.³⁵ nHAp ceramics were characterized by FTIR and SEM. hBMSCs and nHAp interaction was assessed using transmission electron microscopy (TEM).

2.2 | Production and characterization of nanosized hydroxyapatite ceramics

Nano-hydroxyapatite ceramics were produced by wet chemical process as described previously.³⁶ In brief, nHAp particles were precipitated by a reaction between ammonium and calcium nitrate (Ca/P:1.67). The solution was continuously added onto the precipitate and nanoparticles were formed uniformly spherical. Complex-shaped nanoparticles were produced by the uncontrolled precipitation method. The spark plasma method³⁷ at low sintering temperatures was followed for the nanometer-sized bio-ceramic production (Figure S2).

2.2.1 | SEM analysis

The nHAp ceramics were dried at 50°C for 30 min. They were then coated with a thin layer of gold and quantitatively analyzed for their

size, morphology, and content (FEI QUANTA FEG 250). Nanosized HAp ceramic particles produced at 1000°C and sized between 61 \times 50 nm² (Figure S2A,B). The element content analysis by energy-dispersive x-ray spectroscopy (EDX) revealed the Ca-P ratios were 34% and 20%, respectively (Figure S2C).

2.2.2 | FTIR spectroscopy analysis

The nHAp ceramics spectra were recorded with a spectral range of 400–4000 cm⁻¹ (FTIR, Bruker IFS 66/S). Hydroxyapatite showed strong characteristics of P-O tensile and bending absorption bands at 1089, 1023, and 963 cm⁻¹ and at 600 and 561 cm⁻¹. The O–H vibrational vibration was detected with a sharp absorption peak at 3572 cm⁻¹ (Figure S2D).

2.3 | Preparation of rhBMP2 containing nHAp-PEG/PLA

Synthetic biodegradable polymer PEG/PLA (Taki Chemicals Co. Ltd., Japan) was used for the preparation of the composites and the polymeric structure was produced at a PLA: PEG molar ratio of 51:49.^{30,38} rhBMP2 (Taki Chemicals Co., Ltd. and Osteopharma Inc., Japan) was diluted to 1.0 $\mu\text{g}/\text{mL}$ concentration with a buffer (5 mM glutamic acid + 0.5% sucrose + 2.5% glycine + 0.01% Tween 80). The PEG/PLA polymer was liquidized with acetone and rhBMP2 was added to this solution. nHAp ceramics were added into the mix afterwards and the acetone was removed by evaporation within 5 min. rhBMP2 was then combined with the nHAp-PEG/PLA and the final biomaterial was obtained. Release kinetics of rhBMP2 from the composites revealed a burst release that continued for at least 21 days.³⁰

2.4 | Culture and characterization of hBMSCs

A licensed standardized hBMSCs cell line (A15652, #L8900-102, StemPro[®], Gibco) that is internationally validated^{39–43} and GMP-manufactured.⁴⁴ The hBMSCs have been received and expanded in passage 5 that is used for all work packages. The hBMSCs cell line has been validated by the manufacturer for the whole multipotency until passage 7.⁴⁴ Briefly, they were cultured with DMEM-LG (Lonza, Switzerland), 10% FBS (Gibco), 1% Pen-Strep (Lonza, Switzerland) and L-glutamine (HyClone) at 37°C with 5% CO₂ (Figure S3).

Morphological properties and adherence to the culture plates were determined and the potential of osteogenic and chondrogenic differentiation and the surface marker expressions were evaluated.⁴⁵ hBMSCs from passage 5 were used in all experiments. Human BMSCs adhered onto the culture plates within about 12–24 h and fibroblastic spindle-shaped morphology was affirmed (Figure S3A). hBMSCs were trypsinized (Gibco) and seeded 2 \times 10⁵ cells per flow cytometry tube. Cells were incubated with 5.0 μL anti-human CD73, anti-human CD90, anti-human CD45, anti-human HLA-DR (All from

BD Biosciences) at 4°C for 20 min and avoid from the light. Immunolabeling of hBMMSCs was evaluated with the Novocyte (Agilent) device for 15,000 events and results were assessed with the Novo Express (Agilent). Human BMMSCs were positively labeled with anti-CD73 and anti-CD90 and were not label with CD45 and HLA-DR (Figure S3B). hBMMSC were seeded in 24 well plates as 15×10^3 cells/well for the osteogenic differentiation assay.^{46,47} Briefly, the hBMMSCs were supplemented with DMEM-LG, 10 mM β -glycerophosphate (Sigma-Aldrich, Germany), 100 nM dexamethasone (Sigma-Aldrich, Germany), 0.2 mM L-ascorbic acid (Santa Cruz Biotechnology Inc.) and 10% FBS (Gibco) for osteogenic stimulation. On day 21, osteogenic differentiation was assessed by intracellular ALP activity.^{46,47} Briefly, all osteogenic media was removed, substrate solution (SIGMAFAST pNPP, Sigma, Germany) was added instead of osteogenic media, and incubated for 30 min at 37°C in a dark place. The microplate reader (Molecular Devices) measured the absorbance of the whole plate at 405 nm wavelength. hBMMSCs with osteogenic differentiation medium showed higher values than the hBMMSCs, which were cultured with growth medium ($p < 0.001$; Figure S3C). hBMMSCs (25×10^4 cells/tube) were centrifuged at 1,500 rpm during 15 min and the pellet was resuspended with growth medium. After 24 h, the growth medium was removed and DMEM-LG, %0.01 dexamethasone, %1.25 L-ascorbic acid, %1 sodium-pyruvate, 1.0 μ L ITS, 1.0 μ L TGF-3 was added to the forming spheroid pellet for chondrogenic differentiation. On day 21, SOX9 expression was assessed by qPCR. Human BMMSCs were harvested, total RNA was isolated and the RNA purification was evaluated by a spectrophotometer (NanoDrop, Thermo Fisher Scientific). The cDNA synthesis was performed by a cDNA synthesis kit (SCRIPT cDNA Jena Biosciences, Germany) and samples were processed with the ViiA™7 at the qPCR detection system (ThermoFisher Scientific). Expression of SOX9 showed higher values than the hBMMSCs, which were cultured with growth medium ($p < 0.001$; Figure S3D). The manufacturer of hBMMSCs confirmed the adipogenic differentiation profile of these cells (hBMMSCs, #L8900-102, StemPro®, Gibco).

hBMMSCs presented typical spindle shaped morphology, positive expression for CD73 and CD90 and negative expression for CD45 and HLA-DR, optimum chondrogenic and osteogenic differentiation patterns.

2.5 | Proliferation

Effects of rhBMP2 containing nHAp-PEG/PLA on hBMMSCs proliferation were evaluated by real-time quantitative cell analysis system (xCELLigence, Agilent Scientific Instruments). hBMMSCs were seeded as 5×10^3 cells/well in an E-Plate VIEW 96 (Agilent Scientific Instruments) and incubated at 37°C, 5% CO₂ for 21 h. After incubation of hBMMSCs, nHAp-PEG/PLA, 0.5 and 1.0 μ g/mL rhBMP2, 0.5 μ g/mL rhBMP2 + nHAp-PEG/PLA and 1.0 μ g/mL rhBMP2 + nHAp-PEG/PLA were placed into the E-Plate Insert 96 (#C06465382001, Agilent Scientific Instruments) and incubated with hBMMSCs in the same well but separately. The real-time proliferation assessment was performed for 7 days and the cell impedance was measured at every hour.

TABLE 2 Primer sequences were listed.

Primer sequences		
Runx2	Forward	GTTAATCTCCGCAGGTCACT
	Reverse	CACTGTGCTGAAGAGGCTGT
OPN	Forward	TTGCAGCCTTCTCAGCCA
	Reverse	CAAAAGCAAATCACTGCAATTCT
OCN	Forward	CACACTCCTCGCCCTATTG
	Reverse	CGTCCCTCTGCTTG
ACTB	Forward	CGCAAAGACCTGTACGCCAAC
	Reverse	GAGCCGCCGATCCACACG

The time points were determined as 12, 24, 48, and 72 h. Values were normalized to normal culture media.

2.6 | Osteogenic differentiation

Osteogenic differentiation of rhBMP2 containing nHAp-PEG/PLA on hBMMSCs was evaluated by assessing intracellular ALP activity via spectrophotometric assay and early, mid and late osteogenic differentiation markers⁴⁸ (Runx2, OPN, and OCN, respectively) by qPCR.

Human derived BMMSCs (6×10^4 cells/well) were incubated for 24 h at 37°C, 5% CO₂ for the intracellular ALP activity assay. The nHAp-PEG/PLA, 0.5, 1.0, and 3.0 μ g/mL rhBMP2, 0.5 μ g/mL rhBMP2 + nHAp-PEG/PLA, 1.0 μ g/mL rhBMP2 + nHAp-PEG/PLA, and 3.0 μ g/mL rhBMP2 + nHAp-PEG/PLA composites were added to the well. The evaluation of intracellular ALP activity assay was performed on days 3, 10, and 21. According to instructions of manufacturer, the media was removed, substrate solution (SIGMAFAST pNPP, Sigma, Germany) was added into the wells instead of media and incubated for 30 min at 37°C in a dark place. The microplate reader (Molecular Devices) measured the absorbance of the whole plate at 405 nm wavelength.

For qPCR, the Runx2 was analyzed as early marker on day three, OPN as midterm marker on day eight and OCN as late marker on day 21 for 3-week osteogenic differentiation protocol.⁴⁹ The ACTB gene expression was used as the reference gene for normalization. Primer sequences were given in Table 2. The total RNA was isolated from hBMMSCs by TRIzol reagent (Thermo Fisher Scientific). The RNA purification was assessed by a spectrophotometer (NanoDrop, Thermo Fisher). The cDNA was synthesized by a kit (SCRIPT cDNA synthesis kit, Jena Biosciences, Germany). Standard dilutions were prepared, and all samples were processed with the ViiA™7 at the qPCR detection system (Thermo Fisher Scientific) in three replicates. Relative mRNA levels were computed.⁵⁰

2.7 | Morphologic evaluation of hBMMSCs and rhBMP2 containing nHAp-PEG/PLA interaction

Human BMMSCs (10^6 cells/well) were treated with 3.0 μ L rhBMP2 + nHAp-PEG/PLA and incubated at 37°C, with 5% CO₂

for 3 days. For light and transmission electron microscopical evaluation, the medium was removed on day three and hBMMSCs were washed with PBS at room temperature. Then, the cell fixation was performed at 4°C for an hour by %2 glutaraldehyde and cells were post-fixed by osmium tetroxide. The samples were embedded in epon (EMS, Germany), after dehydration with 25%, 50%, 75%, 95%, and 100% (series) ethanol and clearing with propylene oxide. The epon plastic blocks (Agar Scientific, UK) were cut to obtain semi-thin and thin sections. The semi-thin sections were stained with methylene blue-Azur II, the ultra-thin sections were stained with uranyl acetate and lead citrate.

For SEM evaluation, hBMMSCs were fixed with 2% glutaraldehyde solution (Sigma-Aldrich, Germany) at 4°C for an hour on day 3. After fixation, the samples were dehydrated in a series of ethanol. The samples were then dried with a critical point dryer instrument (Tousimis CPD, Autosamdri 815 B) for 30 min and coated with 10 nm gold-palladium by using the Precision Etching Coating System instrument (GATAN 682). Finally, the samples were visualized with SEM (Fei Quanta 200F). EDX analysis showing the surface mineral distribution was also performed in the same device.

2.8 | Statistical analysis

Normality of distribution was evaluated with Shapiro–Wilk test. Kruskal-Wallis and Mann–Whitney U tests were done for comparing non-parametric multiple or two groups of proliferation assay. One-way variance analysis (ANOVA) and Dunn tests were performed for comparing parametric multiple or two groups of ALP activity assays and qPCR, respectively. Descriptive statistics were represented as the mean \pm standard deviation for the parametric tests and median,

minimum-maximum for the nonparametric tests. The significance was accepted as $p < 0.05$. Statistical analyses were conducted with version 21 of IBM SPSS® (IBM).

3 | RESULTS

3.1 | Proliferation

0.5 $\mu\text{g}/\text{mL}$ of rhBMP2 doped on nHAp-PEG/PLA showed highest effect on hBMMSCs proliferation from 48 to 72 h comparing to other rhBMP2 doses and controls with no statistical significance. Thus, proliferative effect of 0.5 $\mu\text{g}/\text{mL}$ rhBMP2 + nHAp-PEG/PLA was similar to that of 1.0 $\mu\text{g}/\text{mL}$ rhBMP2 + nHAp-PEG/PLA at all time points (Figure 1). hBMMSCs proliferation rate increased in time ($p < 0.05$) from until 72 h in 1.0 $\mu\text{g}/\text{mL}$ rhBMP2 + nHAP-PLA/PEG composite group. It increased until 48 h in 0.5 $\mu\text{g}/\text{mL}$ rhBMP2 + nHAP-PLA/PEG composite, the 0.5 $\mu\text{g}/\text{mL}$ rhBMP2 and nHAp-PEG/PLA groups ($p < 0.05$, Figure 1).

3.2 | Osteogenic differentiation

3.2.1 | Alkaline phosphatase activation assay

ALP activity increased ($p < 0.001$) in the 0.5 $\mu\text{g}/\text{mL}$ rhBMP2 + nHAp-PEG/PLA, 1.0 $\mu\text{g}/\text{mL}$ rhBMP2 + nHAp-PEG/PLA and 3.0 $\mu\text{g}/\text{mL}$ rhBMP2 + nHAp-PEG/PLA groups from day 3 to days 10 and 21. On day 3, 3.0 $\mu\text{g}/\text{mL}$ rhBMP2 + nHAp-PEG/PLA composite increased ($p < 0.001$) ALP activity compared to 3.0 $\mu\text{g}/\text{mL}$ rhBMP2, nHAp-PEG/PLA treated groups, negative and positive control groups. ALP activities of the 1.0 $\mu\text{g}/\text{mL}$ rhBMP2 + nHAp-PEG/PLA composite group

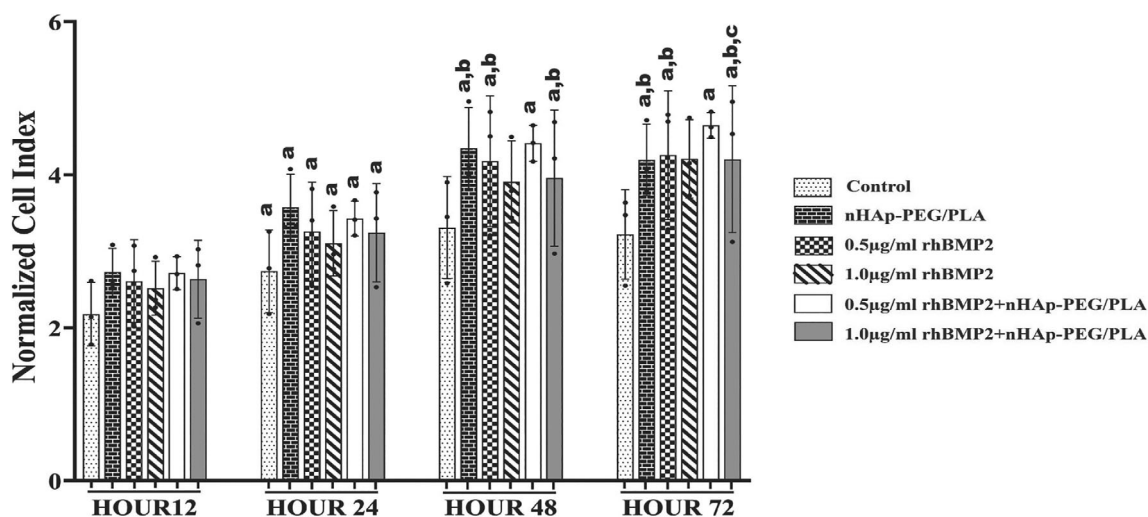


FIGURE 1 Proliferation of hBMMSCs was shown with normalized cell indexes of groups at 12, 24, 48, and 72 h. The lowercase letters a, b and c denote statistically significant ($p < 0.05$) differences compared to 12, 24, and 72 h in same group, respectively. Note that proliferative effect of 0.5 $\mu\text{g}/\text{mL}$ rhBMP2 + nHAp-PEG/PLA is highest comparing to other groups on 48 and 72 h but not statistically significant. (●) represents individual scatters of the samples ($n = 3$).

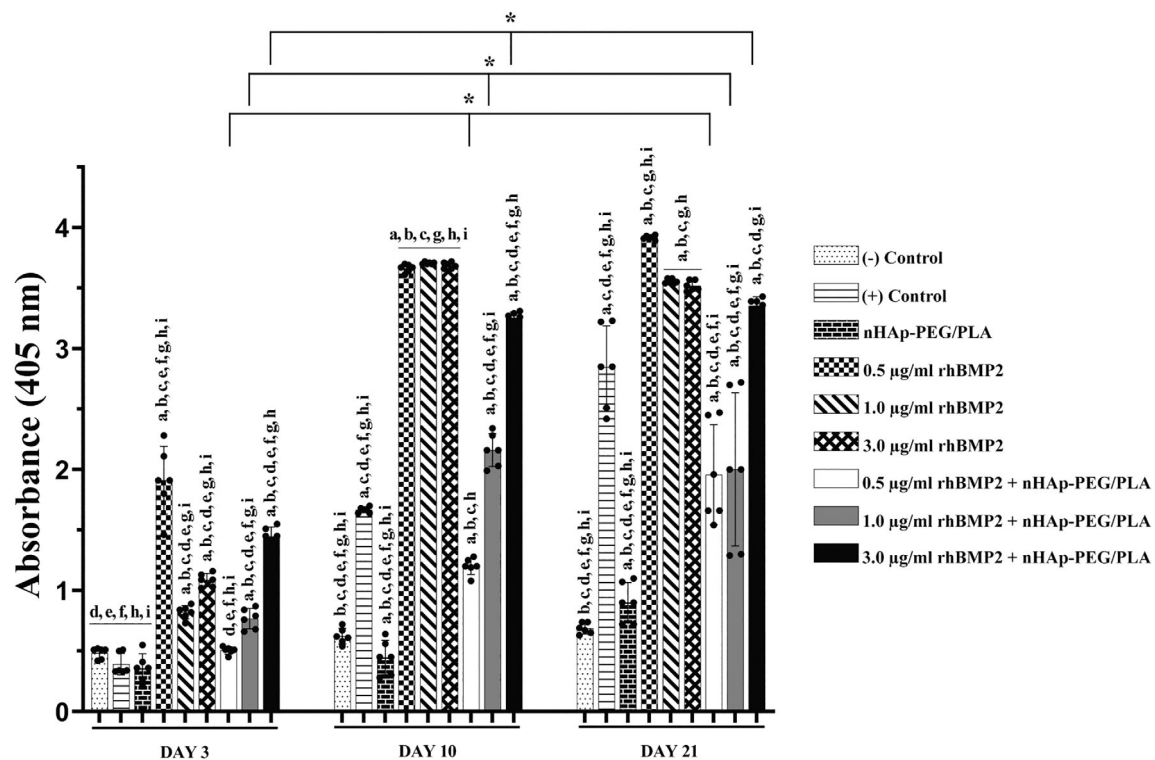


FIGURE 2 Osteogenic differentiation of hBMMSCs was shown with ALP activity of groups on days 3, 10, and 21. The lowercase letters a, b, c, d, e, f, g, h, and i denote statistically significant ($p < 0.05$) differences compared to (-) control, (+) control, nHAp-PEG/PLA, 0.5 $\mu\text{g}/\text{mL}$ rhBMP2, 1.0 $\mu\text{g}/\text{mL}$ rhBMP2, 3.0 $\mu\text{g}/\text{mL}$ rhBMP2, 0.5 $\mu\text{g}/\text{mL}$ rhBMP2 + nHAp-PEG/PLA, 1.0 $\mu\text{g}/\text{mL}$ rhBMP2 + nHAp-PEG/PLA, 3.0 $\mu\text{g}/\text{mL}$ rhBMP2 + nHAp-PEG/PLA groups in same time point, respectively. * $p < 0.05$ change in groups depending on time. (●) represents individual scatters of the samples ($n = 6$).

was higher ($p < 0.001$) than nHAp-PEG/PLA treated group, negative and positive control groups on day 3. 0.5 $\mu\text{g}/\text{mL}$ rhBMP2 + nHAp-PEG/PLA composite did not affect ALP activity of hBMMSCs on day 3. On day 10, 1.0 $\mu\text{g}/\text{mL}$ rhBMP2 + nHAp-PEG/PLA and 3.0 $\mu\text{g}/\text{mL}$ rhBMP2 + nHAp-PEG/PLA composites increased ($p < 0.001$) ALP activity compared nHAp-PEG/PLA treated groups negative and positive control groups. The 0.5 $\mu\text{g}/\text{mL}$ rhBMP2 + nHAp-PEG/PLA composite group induced ($p < 0.05$) ALP activity of hBMMSCs compared to nHAp-PEG/PLA treated and negative control groups on day 10. On day 21, 0.5, 1.0 and 3.0 $\mu\text{g}/\text{mL}$ rhBMP2 + nHAp-PEG/PLA composite groups increased ALP activity compared to nHAp-PEG/PLA treated and negative control groups ($p < 0.001$, Figure 2).

3.2.2 | qPCR

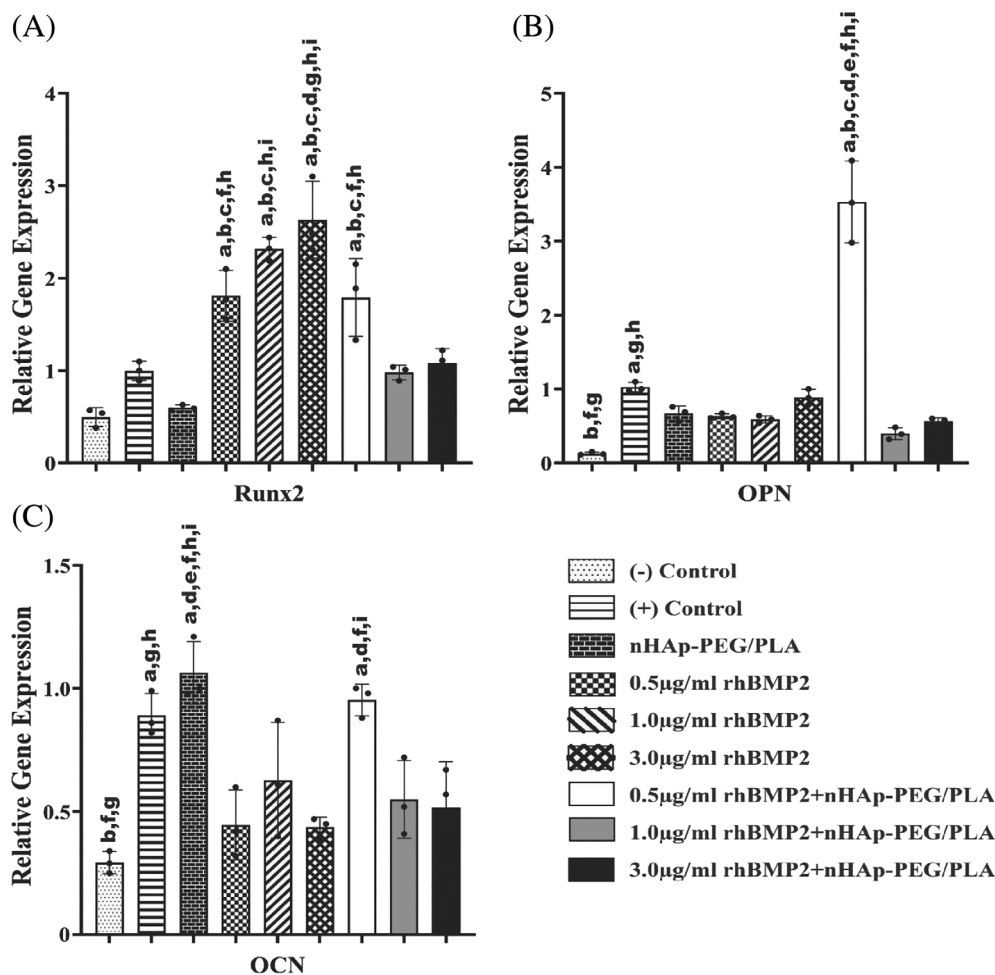
The 0.5 $\mu\text{g}/\text{mL}$ rhBMP2 + nHAp-PEG/PLA composite group increased Runx2 expression compared to the nHAp-PEG/PLA composite ($p < 0.001$) and the positive control ($p = 0.021$) groups. Runx2 expressions of the hBMMSCs increased in the 0.5, 1.0, and 3.0 $\mu\text{g}/\text{mL}$ rhBMP2 ($p = 0.017$, $p < 0.001$, $p < 0.001$, respectively) groups compared to the positive control group. OPN expression of the hBMMSCs increased ($p < 0.001$) in the 0.5 $\mu\text{g}/\text{mL}$ rhBMP2 + nHAp-PEG/PLA composite groups compared to the nHAp-PEG/PLA, the positive

control and the 0.5, 1.0, and 3.0 $\mu\text{g}/\text{mL}$ rhBMP2 groups. The 1.0 $\mu\text{g}/\text{mL}$ rhBMP2 + nHAp-PEG/PLA decreased OPN expression of hBMMSCs compared to the positive control group ($p < 0.05$). The 0.5 $\mu\text{g}/\text{mL}$ rhBMP2 + nHAp-PEG/PLA group increased OCN expression of hBMMSCs compared to the 0.5 $\mu\text{g}/\text{mL}$ and the 3.0 $\mu\text{g}/\text{mL}$ rhBMP2 groups ($p = 0.007$, $p = 0.025$, respectively). OCN expression of the positive control group was higher ($p < 0.05$) than that of the 0.5 and 3.0 $\mu\text{g}/\text{mL}$ rhBMP2 groups (Figure 3). Thus, inductive effect of 0.5 $\mu\text{g}/\text{mL}$ rhBMP2 + nHAp-PEG/PLA was superior to that of 1.0 and 3 $\mu\text{g}/\text{mL}$ rhBMP2 + nHAp-PEG/PLA on osteogenic gene expression (Figure 3).

3.3 | hBMMSCs and nHAp-PEG/PLA containing rhBMP2 were in close contact

The hBMMSCs presented ovoid or stellate shape morphology with a centrally located euchromatic nucleus, single or double nucleoli, enlarged endoplasmic reticulum cisternae and numerous cytoplasmic vacuoles under TEM. They exhibited multiple cytoplasmic projections and appeared to be in close contact with the composite particles. Composite particles attached to each other, formed clusters and adhered to the culture plates. They formed huge superposed masses with hBMMSCs or presented as nanoparticles in the vacuoles of the

FIGURE 3 Osteogenic differentiation as relative (A) Runx2, (B) OPN, and (C) OCN expressions were shown by qPCR evaluation. The lowercase letters a, b, c, d, e, f, g, h, and i denote statistically significant ($p < 0.05$) differences compared to (-) control, (+) control, nHAp-PEG/PLA, 0.5 $\mu\text{g}/\text{mL}$ rhBMP2, 1.0 $\mu\text{g}/\text{mL}$ rhBMP2, 3.0 $\mu\text{g}/\text{mL}$ rhBMP2, 0.5 $\mu\text{g}/\text{mL}$ rhBMP2 + nHAp-PEG/PLA, 1.0 $\mu\text{g}/\text{mL}$ rhBMP2 + nHAp-PEG/PLA, 3.0 $\mu\text{g}/\text{mL}$ rhBMP2 + nHAp-PEG/PLA groups, respectively. Note that the osteogenic effect of 0.5 $\mu\text{g}/\text{mL}$ rhBMP2 + nHAp-PEG/PLA is superior that of 1.0 and 3 $\mu\text{g}/\text{mL}$ rhBMP2 + nHAp-PEG/PLA on Runx2, OPN, and OCN gene expression. 1.0 and 3 $\mu\text{g}/\text{mL}$ rhBMP2 + nHAp-PEG/PLA act similarly. (●) represents individual scatters of the samples ($n = 3$).



cytoplasmic extensions of cells that have increased vesicular traffic within their endo-lysosomal compartments (Figure 4A-C).

PEG/PLA particles were amorphous and nHAp particles presented homogeneous crystal structures (Figure 4D) under SEM. At least one dimension of the nHAp crystals was in the nanometer scale (Figure 4E). hBMMSCs exhibited oval or spindle shaped morphology with cytoplasmic projections adjacent to and/or attached to the nanobiomaterial pores (Figure 4E,F). The high-density distribution of Ca and P indicated the presence of nanosized hydroxyapatite, while O, P, and N the hBMMSCs by EDX elemental analysis (Figure 4G).

4 | DISCUSSION

We hypothesized that 0.5, 1.0, and 3.0 $\mu\text{g}/\text{mL}$ rhBMP2 + nHAp-PEG/PLA composites will stimulate proliferation and osteogenic differentiation of hBMMSCs. These composites can then be used in PLSF when the appropriate dose of application could be optimized. We therefore developed a novel composite of rhBMP2 containing nHAp-PEG/PLA³⁰ and evaluated its proliferation and osteogenic differentiation potential on hBMMSCs previously. Real time cell analysis demonstrated the hBMMSC proliferation capacity with these composites. The 0.5 $\mu\text{g}/\text{mL}$ rhBMP2 group had the highest proliferative capacity.

The 3.0 $\mu\text{g}/\text{mL}$ rhBMP2 + nHAp-PEG/PLA composite group presented higher ALP activity in all times when compared to the other groups. The 0.5 $\mu\text{g}/\text{mL}$ rhBMP2 + nHAp-PEG/PLA composite group presented the highest expression rate for Runx2, OCN, and OPN according to our qPCR results.

Peaks of P-O and O-H bands appeared at 1089, 1023, 963, 600, 561, and 3572 cm^{-1} , respectively in FTIR and characteristic bands of nHAp were detected during the characterization of the composites. A previous study⁵¹ reported that the P-O and the O-H bands appeared at 1086, 1030, 962, and 3570 cm^{-1} , 630 cm^{-1} , while another study⁵¹ stated that the P-O band was detected at 1092, 1023, and 963 cm^{-1} . Our SEM and EDX evaluations showed that the produced nHAp was nano sized and had 34% of Ca and 20% of P content. SEM and EDX findings proved that the nHAp that was produced for this study was in compliance with the literature⁵¹⁻⁵⁴ and may have osteoconductive properties.

In our study, hBMMSCs proliferated from 12 to 48 h when combined with 0.5 $\mu\text{g}/\text{mL}$ rhBMP2 + nHAp-PEG/PLA, and to 72 h when combined with 1.0 $\mu\text{g}/\text{mL}$ rhBMP2 + nHAp-PEG/PLA. 0.5 $\mu\text{g}/\text{mL}$ of rhBMP2 generated similar real time proliferation rates on hBMMSCs when doped to nHAp-PEG/PLA comparing to higher dose (1.0 $\mu\text{g}/\text{mL}$ rhBMP2 + nHAp-PEG/PLA). Composites containing rhBMP2 in previous studies^{21-23,28-32} revealed conflicting MSC proliferation results

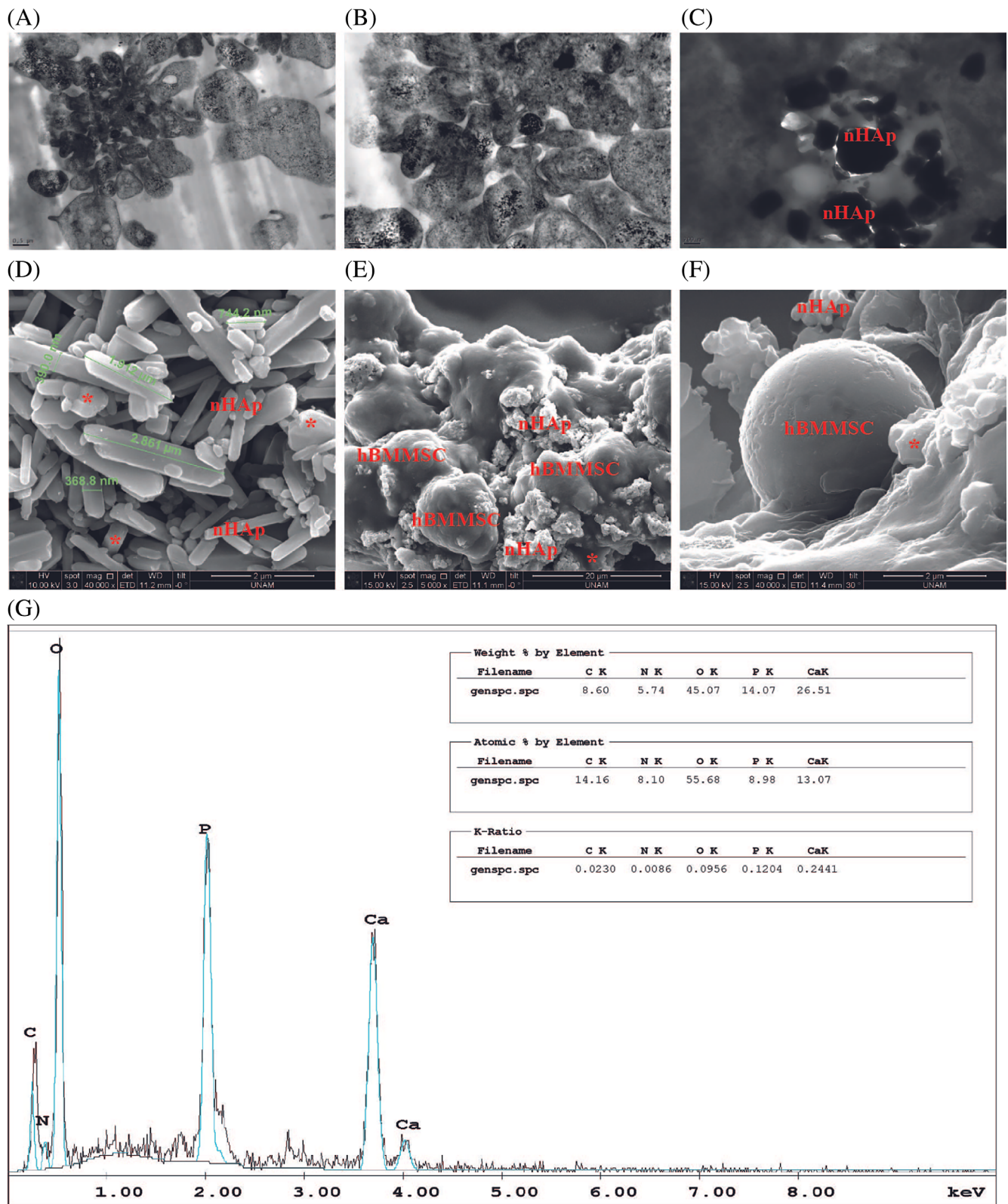


FIGURE 4 (A, B, C) Transmission electron micrographs show the nanoceramic particles taken into the cytoplasmic extensions of hBMSCs, uranyl acetate, lead citrate (A) 30 000 \times , (B) 50 000 \times , (C) 60 000 \times . (D, E, F) Scanning electron micrographs present the hBMSCs superposed with nHAp-PEG/PLA on day 3, (D) 40 000 \times , (E) 5000 \times , (F) 40 000 \times . (G) EDX mineral distribution graphic of rhBMP2 containing nHAp-PEG/PLA with hBMSCs. nHAp-PEG/PLA and hBMSCs with nHAp and PEG/PLA were visualized by SEM on day 3 (E, F). (*) shows nHAP-PEG/PLA composite.

for different doses (Table S1). PEG/PLA-dexamethasone containing 5.0 µg of rhBMP2 increased proliferation of rat BMSCs when compared to the PEG/PLA-dexamethasone group on day four by live and dead cells assay.¹⁹ 25 µg rhBMP coated silk scaffold stimulated proliferation of hBMMSCs on day 5³³ and 0.3 ng/mL rhBMP2 containing nHAp-PLGA nanofibrous scaffolds increased the proliferation of mouse MC3T3-E1 pre-osteoblastic cells on day 6.²¹ Our proliferative dose range within the composite is in line with previous studies revealing 0.5 µg/mL being effective when doped into nHAp-PLA/PEG. We previously reported rhBMP2 release from nHAp-PLA/PEG as 3%–6% in 21 days.³⁰ Our data are consistent with the previous studies.^{19,21,33}

Osteogenic differentiation assays showed that the 3.0 µg/mL rhBMP2 + nHAp-PEG/PLA composites increased ALP activity on days 3, 10, and 21. OCN, Runx2, and OPN expressions increased in the 0.5 µg/mL rhBMP2 + nHAp-PEG/PLA composite group. In previous studies,^{21–23,28,29,31,32} ALP activity and qPCR methods were used to determine osteogenic differentiation by rhBMP2. Different rhBMP2 doses were however not examined for osteogenic differentiation. Our study that evaluated the dose-effect was in line with the literature (Table S1). The 1 µg rhBMP2-loaded HAp/beta-tricalcium phosphate microsphere/hydrogel composite induced ALP activity, OCN, Runx2 and OPN expressions on MC3T3 pre-osteoblast cells from days 7 to 14.³¹ The nHAp-collagen-PLA containing 0.1³² and 200 µg/mL²³ rhBMP2 composites increased ALP activity, OCN, Runx2, OPN, ALP, and collagen 1 (COL1) expressions of human amnion derived MSCs and rat BMMSCs, respectively, from day 7 to 21. PLGA-PEG-COOH microparticles loaded with 20 µg/mL rhBMP2 encapsulated in a nHAp-PLGA scaffold containing the encapsulated PLGA-PEG-COOH microparticles loaded with 20 µg/mL rhBMP2 induced ALP activity from days 14 to 21.²⁹ nHAp-Silk-fibroin scaffolds containing 0.2–250 µg/mL rhBMP2 also increased ALP activity^{22,28} and OCN, ALP, COL1 and Runx2 expressions²⁸ of rat BMMSCs from days 7 to 14. The increase in ALP activity and osteogenic genes OCN, Runx2, and OPN expression were evident in the rhBMP2 groups. nHAp-PEG/PLA alone was not sufficient in stimulating the ALP activity in our study. rhBMP2 in between 0.0003 and 200 µg/mL doses increased extracellular mineralization and osteogenic differentiation (Table S2). In previous studies (Table S2), this increase was monitored by ALP activity and expression rates of osteogenic differentiation-related genes which were Runx2, OPN, OCN, COL1, and ALP on the MSCs in a week to 4 weeks. We evaluated ALP activity on days 3, 10, and 21 and Runx2, OPN, and OCN on days 3, 8, and 21. All rhBMP2 containing composites increased Runx2 when compared to the control group in our study. Increasing the rhBMP2 dose from 1.0 to 3.0 µg/mL, however, did not change the Runx2 expression. This however was only observed in the 0.5 µg/mL rhBMP2 + nHAp-PEG/PLA composite group for OPN and for the 1.0 µg/mL rhBMP2 + nHAp-PEG/PLA composite group for OCN. We, therefore, conclude that 0.5 µg/mL rhBMP2 having a release rate as 3%–6% (in 21 days) from nHAp-PLA/PEG composite is adequate to stimulate mesenchymal stem cell proliferation until 3 days. Same dose induces also expression of early (Runx2), medium (OPN) and late (OCN) term osteogenic

markers on days 3, 7, and 10, respectively. However, 0.5 µg/mL of rhBMP2 within the composite has not been enough to induce ALP activity as an early indicator of extracellular matrix synthesis.

Combining synthetic grafts with MSCs and BMP is a challenging issue as the synergistic effect of each of the components may stimulate proliferation and differentiation in PLSF as it was observed in our previous study.³⁰ Our findings were partially in line with two other studies.^{19,31} PEG/PLA-dexamethasone containing 5.0 µg of rhBMP2 increased proliferation of rat BMSCs when compared to the PEG/PLA-dexamethasone group on day four by live and dead cells assay¹⁹ 0.5 µg rhBMP2 however did not change the proliferation of MC3T3 cells from 12 to 72 h by the CCK-8 proliferation assay in another study.³¹ These studies did not compare outcomes with different doses of BMP2. Polymer-based composites containing 0.5 µg/mL rhBMP2 did not change proliferation but osteogenic differentiation of hBMSCs and MC3T3 cells.³¹ 5.0 µg/mL rhBMP2 increased proliferation and differentiation of MSCs¹⁹ as we observed in this current study. Our group previously reported that 3 µg/mL rhBMP2 doped nHAp-PEG/PLA presented similar spinal fusion rate and increased bone volume on week 8 comparing to higher dose (10 µg/mL doped nHAp-PEG/PLA) by manual palpation, µCT and histology when applied in vivo to lumbar 4–5 vertebrae rat PLSF model. Our findings were in line with a recent study¹⁴ that evaluated fusion in non-human primates. Our dose window is in line with previous in vitro studies^{21–23,28,29,31,32} revealing that optimal beneficial osteogenic effect of rhBMP2 takes place within a very tight dose window that would cause no inflammation but osteoinduction when applied to in vivo setting including lumbar spinal fusion model.³⁰ Systemic dose of rhBMP2 that is doped into nHAP-PLA/PEG was higher in our previous in vivo animal model when compared to present in vitro molecular experiment setting and demonstrated that a lower dose may be efficient to induce proliferation and ossification of stem/progenitor osteogenic cells (MSCs).

This study has several limitations. hBMMSCs but no osteoblasts were examined. Additionally, the hBMMSCs were from a single but licensed, standardized commercial cell line belonging to one donor. However, the hBMMSCs cell line has been widely used as a single test line in previous studies^{39–43} that proved the validity of the line and did not interfere with our aims as MSCs are precursors of osteogenic and chondrogenic cells in this pilot study. Results of osteogenic differentiation assays were restricted to four biomarkers and three time points. Adding nHAp-PEG/PLA into the real-time quantitative cell analysis system may have deteriorative effects for quantifying cellular proliferation.

In conclusion, this study revealed the effects of a novel rhBMP2 + HAp-PLA/PEG composite on the in vitro proliferation and osteogenic differentiation of hBMMSCs. Previous pre-clinical studies have used a dose range in between 5.0 and 50.0 µg of BMP2 for bone regeneration¹⁹ and spinal fusion.^{13,30} However we were able to present proliferation and differentiation with 0.5 and 1.0 µg/mL BMP2 doses when combined with nHAP-PEG/PLA. Our in vitro results suggest that 0.5 and 1.0 µg/ml BMP2 doses when combined with nHAP-PEG/PLA could enhance PLSF results.

AUTHOR CONTRIBUTIONS

Petek Korkusuz, Feza Korkusuz, and Takashi Kaito created the idea. Eda Çiftci Dede and Merve Gizer performed the experiments. Eda Çiftci Dede, Merve Gizer, Feza Korkusuz, and Petek Korkusuz collected data and analyzed the outcomes. Eda Çiftci Dede, Merve Gizer, Petek Korkusuz, Feza Korkusuz, Zeynep Bal, Hiroyuki Ishiguro, Hideki Yoshikawa, and Takashi Kaito wrote the paper. Petek Korkusuz supervised the work.

ACKNOWLEDGMENTS

TÜBİTAK and JSPS funded this study (Project no: 215S834). Authors would like to thank Beren Karaosmanoğlu, Ekim Taşkıran, Selin Önen, Özge Boyacıoğlu, Berna Kankılıç, Çağla Köprü, Şebnem Şahin, Masafumi Kashii, Takashiro Makino, Sadaaki Kanayama, Kunihiro Hashimoto, Tokimitsu Morimoto, Rintaro Okada, Junichi Kushioka, Ryota Chijimatsu, Joe Kodama, Daisuke Tateiwa, Yuichiro Ukon, and Shinichi Nakagawa for their contributions to this study. Feza Korkusuz MD is an active member of the Turkish Academy of Sciences (TUBA).

CONFLICT OF INTEREST STATEMENT

Takashi Kaito is an Editorial Board member of JOR Spine and a co-author of this article. To minimize bias, they were excluded from all editorial decision-making related to the acceptance of this article for publication. [Correction added on 23 June 2023, after first online publication: Conflict of Interest statement was revised]

ORCID

Eda Çiftci Dede  <https://orcid.org/0000-0001-6900-4702>

Merve Gizer  <https://orcid.org/0000-0003-1911-2363>

Takashi Kaito  <https://orcid.org/0000-0003-4882-2997>

Petek Korkusuz  <https://orcid.org/0000-0002-7553-3915>

REFERENCES

- Plantz MA, Gerlach EB, Hsu WK. Synthetic bone graft materials in spine fusion: current evidence and future trends. *Int J Spine Surg.* 2021;15:104-112. doi:10.14444/8058
- Chiarello E, Cadossi M, Tedesco G, et al. Autograft, allograft and bone substitutes in reconstructive orthopedic surgery. *Aging Clin Exp Res.* 2013;25(1):S101-S103. doi:10.1007/s40520-013-0088-8
- Moraschini V, Almeida DCF, Calasans-Maia MD, Kischinhevsky ICC, Louro RS, Granjeiro JM. Immunological response of allogeneic bone grafting: a systematic review of prospective studies. *J Oral Pathol Med.* 2020;49:395-403. doi:10.1111/jop.12998
- Brink O. The choice between allograft or demineralized bone matrix is not unambiguous in trauma surgery. *Injury.* 2021;52(2):S23-S28. doi:10.1016/j.injury.2020.11.013
- Zhang Y, Jiang Y, Zou D, Yuan B, Ke HZ, Li W. Therapeutics for enhancement of spinal fusion: a mini review. *J Orthop Translat.* 2021; 31:73-79. doi:10.1016/j.jot.2021.11.001
- Zhang H, Dial B, Brown C. Early fusion rates after direct lateral lumbar Interbody fusion with bone-morphogenetic protein. *Int J Spine Surg.* 2021;15:423-428. doi:10.14444/8063
- Tannoury CA, An HS. Complications with the use of bone morphogenetic protein 2 (BMP-2) in spine surgery. *Spine J.* 2014;14:552-559. doi:10.1016/j.spinee.2013.08.060
- Lykissas M, Gkiatas I. Use of recombinant human bone morphogenetic protein-2 in spine surgery. *World J Orthop.* 2017;8:531-535. doi:10.5312/wjo.v8.i7.531
- Bal Z, Kushioka J, Kodama J, et al. BMP and TGFβ use and release in bone regeneration. *Turk J Med Sci.* 2020;50:1707-1722. doi:10.3906/sag-2003-127
- Arzeno A, Wang T, Huddleston JI. Abundant heterotopic bone formation following use of rhBMP-2 in the treatment of acetabular bone defects during revision hip arthroplasty. *Arthroplast Today.* 2018;4: 162-168. doi:10.1016/j.artd.2017.12.004
- Woo EJ. Adverse events after recombinant human BMP2 in nonspinal orthopaedic procedures. *Clin Orthop Relat Res.* 2013;471:1707-1711. doi:10.1007/s11999-012-2684-x
- James AW. Review of signaling pathways governing MSC osteogenic and adipogenic differentiation. *Scientifica (Cairo).* 2013;2013:684736. doi:10.1155/2013/684736
- Hu T, Liu L, Lam RWM, et al. Bone marrow mesenchymal stem cells with low dose bone morphogenetic protein 2 enhances scaffold-based spinal fusion in a porcine model. *J Tissue Eng Regen Med.* 2022; 16:63-75. doi:10.1002/term.3260
- Seeherman HJ, Wilson CG, Vanderploeg EJ, et al. A BMP/activin a chimera induces posterolateral spine fusion in nonhuman primates at lower concentrations than BMP-2. *JBJS.* 2021;103:e64. doi:10.2106/jbjs.20.02036
- Ma D, An G, Liang M, Liu Y, Zhang B, Wang Y. A composited PEG-silk hydrogel combining with polymeric particles delivering rhBMP-2 for bone regeneration. *Mater Sci Eng C.* 2016;65:221-231. doi:10.1016/j.msec.2016.04.043
- Aoki K, Saito N. Biodegradable polymers as drug delivery systems for bone regeneration. *Pharmaceutics.* 2020;12:95. doi:10.3390/pharmaceutics12020095
- Senra MR, Marques M. Synthetic polymeric materials for bone replacement. *J Compos Sci.* 2020;4:191.
- Brunello G, Panda S, Schiavon L, Sivoletta S, Biasetto L, Del Fabbro M. The impact of bioceramic scaffolds on bone regeneration in preclinical In vivo studies: a systematic review. *Materials (Basel).* 2020;13: 1500. doi:10.3390/ma13071500
- Wu Z, Bao C, Zhou S, et al. The synergetic effect of bioactive molecule-loaded electrospun core-shell fibres for reconstruction of critical-sized calvarial bone defect-the effect of synergetic release on bone formation. *Cell Prolif.* 2020;53:e12796. doi:10.1111/cpr.12796
- Syvänen J, Nietosvaara Y, Kohonen I, et al. Treatment of aneurysmal bone cysts with bioactive glass in children. *Scand J Surg.* 2018;107: 76-81. doi:10.1177/1457496917731185
- He J, Jiang N, Qin T, et al. Microfiber-reinforced nanofibrous scaffolds with structural and material gradients to mimic ligament-to-bone interface. *J Mater Chem B.* 2017;5:8579-8590. doi:10.1039/c7tb02089a
- Niu B, Li B, Gu Y, Shen X, Liu Y, Chen L. In vitro evaluation of electrospun silk fibroin/nano-hydroxyapatite/BMP-2 scaffolds for bone regeneration. *J Biomater Sci Polym Ed.* 2017;28:257-270. doi:10.1080/09205063.2016.1262163
- Wu S, Xiao Z, Song J, Li M, Li W. Evaluation of BMP-2 enhances the osteoblast differentiation of human amnion mesenchymal stem cells seeded on nano-hydroxyapatite/collagen/poly(L-lactide). *Int J Mol Sci.* 2018;19:2171. doi:10.3390/ijms19082171
- Chen Z, Zhang Z, Feng J, et al. Influence of mussel-derived bioactive BMP-2-decorated PLA on MSC behavior in vitro and verification with osteogenicity at ectopic sites in vivo. *ACS Appl Mater Interfaces.* 2018;10:11961-11971. doi:10.1021/acsami.8b01547
- Zhang X, Lou Q, Wang L, Min S, Zhao M, Quan C. Immobilization of BMP-2-derived peptides on 3D-printed porous scaffolds for enhanced osteogenesis. *Biomed Mater.* 2019;15:015002. doi:10.1088/1748-605X/ab4c78

26. Cheng CH, Chen YW, Kai-Xing Lee A, Yao CH, Shie MY. Development of mussel-inspired 3D-printed poly(lactic acid) scaffold grafted with bone morphogenetic protein-2 for stimulating osteogenesis. *J Mater Sci Mater Med*. 2019;30:78. doi:10.1007/s10856-019-6279-x
27. Ye K, Liu D, Kuang H, et al. Three-dimensional electrospun nanofibrous scaffolds displaying bone morphogenetic protein-2-derived peptides for the promotion of osteogenic differentiation of stem cells and bone regeneration. *J Colloid Interface Sci*. 2019;534:625-636. doi:10.1016/j.jcis.2018.09.071
28. Qiu Y, Xu X, Guo W, Zhao Y, Su J, Chen J. Mesoporous hydroxyapatite nanoparticles mediate the release and bioactivity of BMP-2 for enhanced bone regeneration. *ACS Biomater Sci Eng*. 2020;6:2323-2335. doi:10.1021/acsbomaterials.9b01954
29. Kang F, Yi Q, Gu P, et al. Controlled growth factor delivery system with osteogenic-angiogenic coupling effect for bone regeneration. *J Orthop Transl*. 2021;31:110-125. doi:10.1016/j.jot.2021.11.004
30. Bal Z, Korkusuz F, Ishiguro H, et al. A novel nano-hydroxyapatite/synthetic polymer/bone morphogenetic protein-2 composite for efficient bone regeneration. *Spine J*. 2021;21:865-873. doi:10.1016/j.spinee.2021.01.019
31. Tateiwa D, Nakagawa S, Tsukazaki H, et al. A novel BMP-2-loaded hydroxyapatite/beta-tricalcium phosphate microsphere/hydrogel composite for bone regeneration. *Sci Rep*. 2021;11:16924. doi:10.1038/s41598-021-96484-4
32. E LL, Zhang R, Li CJ, et al. Effects of rhBMP-2 on bone formation capacity of rat dental stem/progenitor cells from dental follicle and alveolar bone marrow. *Stem Cells Dev*. 2021;30:441-457. doi:10.1089/scd.2020.0170
33. Jin SK, Lee JH, Hong JH, Park JK, Seo YK, Kwon SY. Enhancement of osseointegration of artificial ligament by nano-hydroxyapatite and bone morphogenetic protein-2 into the rabbit femur. *Tissue Eng Regen Med*. 2016;13:284-296. doi:10.1007/s13770-016-9051-z
34. Köse S, Kankilic B, Gizer M, et al. *Novel Biomaterials for Regenerative Medicine*. Springer; 2018:317-342.
35. Bustin SA, Benes V, Garson JA, et al. The MIQE guidelines: minimum information for publication of quantitative real-time PCR experiments. *Clin Chem*. 2009;55:611-622. doi:10.1373/clinchem.2008.112797
36. Ciftci E, Köse S, Korkusuz P, Timuçin M, Korkusuz F. Boron containing Nano hydroxyapatites (B-n-HAp) stimulate mesenchymal stem cell adhesion. *Key Eng Mater*. 2015;631:373-378. doi:10.4028/www.scientific.net/KEM.631.373
37. Guo X, Xiao P, Liu J, Shen Z. Fabrication of nanostructured hydroxyapatite via hydrothermal synthesis and spark plasma sintering. *J Am Ceram Soc*. 2005;88:1026-1029. doi:10.1111/j.1551-2916.2005.00198.x
38. Kaito T, Myoui A, Takaoka K, et al. Potentiation of the activity of bone morphogenetic protein-2 in bone regeneration by a PLA-PEG/hydroxyapatite composite. *Biomaterials*. 2005;26:73-79. doi:10.1016/j.biomaterials.2004.02.010
39. Kim H-S, Jang JH, Oh JS, Lee EJ, Han CM, Shin US. Injectable remodeling hydrogels derived from alendronate-tethered alginate calcium complex for enhanced osteogenesis. *Carbohydr Polym*. 2023;303:120473.
40. Lyu Z, Park J, Kim KM, et al. A neurovascular-unit-on-a-chip for the evaluation of the restorative potential of stem cell therapies for ischaemic stroke. *Nat Biomed Eng*. 2021;5:847-863.
41. Janarthanan G, Tran HN, Cha E, Lee C, das D, Noh I. 3D printable and injectable lactoferrin-loaded carboxymethyl cellulose-glycol chitosan hydrogels for tissue engineering applications. *Mater Sci Eng C*. 2020;113:111008.
42. Afzal J, Chan A, Karakas MF, et al. Cardiosphere-derived cells demonstrate metabolic flexibility that is influenced by adhesion status. *Basic Transl Sci*. 2017;2:543-560.
43. Canali C, Heiskanen A, Muhammad HB, et al. Bioimpedance monitoring of 3D cell culturing—complementary electrode configurations for enhanced spatial sensitivity. *Biosens Bioelectron*. 2015;63:72-79.
44. ThermoFisherScientific. StemPro™ BM Mesenchymal Stem Cells, January 27, 2023, <https://www.thermofisher.com/order/catalog/product/A15652>.
45. Dominici M, le Blanc K, Mueller I, et al. Minimal criteria for defining multipotent mesenchymal stromal cells. The International Society for Cellular Therapy position statement. *Cytotherapy*. 2006;8:315-317. doi:10.1080/14653240600855905
46. Gizer M, Köse S, Karaosmanoglu B, et al. The effect of boron-containing nano-hydroxyapatite on bone cells. *Biol Trace Elem Res*. 2020;193:364-376. doi:10.1007/s12011-019-01710-w
47. Çiftci Dede E, Korkusuz P, Bilgiç E, Çetinkaya MA, Korkusuz F. Boron nano-hydroxyapatite composite increases the bone regeneration of ovariectomized rabbit femurs. *Biol Trace Elem Res*. 2022;200:183-196. doi:10.1007/s12011-021-02626-0
48. Huang Z, Nelson ER, Smith RL, Goodman SB. The sequential expression profiles of growth factors from osteoprogenitors [correction of osteoprogenitors] to osteoblasts in vitro. *Tissue Eng*. 2007;13:2311-2320. doi:10.1089/ten.2006.0423
49. Kulterer B, Friedl G, Jandrositz A, et al. Gene expression profiling of human mesenchymal stem cells derived from bone marrow during expansion and osteoblast differentiation. *BMC Genom*. 2007;8:70.
50. Rao X, Huang X, Zhou Z, Lin X. An improvement of the 2(-delta delta CT) method for quantitative real-time polymerase chain reaction data analysis. *Biostat Bioinforma Biomath*. 2013;3:71-85.
51. Bakan F. A systematic study of the effect of pH on the initialization of Ca-deficient hydroxyapatite to β -TCP nanoparticles. *Materials (Basel)*. 2019;12:354. doi:10.3390/ma12030354
52. Fan J, Yu MY, Lei TD, et al. In vivo biocompatibility and improved compression strength of reinforced keratin/hydroxyapatite scaffold. *Tissue Eng Regen Med*. 2018;15:145-154. doi:10.1007/s13770-017-0083-9
53. PremVictor S, Kunnumpurathu J, Gayathri devi MG, Remya K, Vijayan VM, Muthu J. Design and characterization of biodegradable macroporous hybrid inorganic-organic polymer for orthopedic applications. *Mater Sci Eng C*. 2017;77:513-520. doi:10.1016/j.msec.2017.03.171
54. Ruixin L, Cheng X, Yingjie L, et al. Degradation behavior and compatibility of micro, nanoHA/chitosan scaffolds with interconnected spherical macropores. *Int J Biol Macromol*. 2017;103:385-394. doi:10.1016/j.ijbiomac.2017.03.175

SUPPORTING INFORMATION

Additional supporting information can be found online in the Supporting Information section at the end of this article.

How to cite this article: Dede, E. Ç., Gizer, M., Korkusuz, F., Bal, Z., Ishiguro, H., Yoshikawa, H., Kaito, T., & Korkusuz, P. (2023). A pilot study: Nano-hydroxyapatite-PEG/PLA containing low dose rhBMP2 stimulates proliferation and osteogenic differentiation of human bone marrow derived mesenchymal stem cells. *JOR Spine*, 6(3), e1258. <https://doi.org/10.1002/jsp2.1258>